Modeling of hyperthermia induced by functionalized gold nanorods bound to Staphylococcus aureus under NIR laser radiation

Alexander N. Yakunin,[a,1] Sergey V. Zarkov,[a] Yuri A. Avetisyan,[a]
Garif G. Akchurin,[a,b] Georgy G. Akchurin Jr.,[a,b] Elena S. Tuchina,[b] Valery V. Tuchin,[a,b,c]

[a]Institute of Precision Mechanics and Control, Russian Academy of Sciences, 24 Rabochaya str., Saratov 410028, Russia; [b]Saratov State University, 83 Astrakhanskaya str., Saratov 410012, Russia; [c]Tomsk State University, 36 Lenin ave., Tomsk 634050, Russia

ABSTRACT

In this paper, a theoretical model of the formation of a local temperature field in suspensions of microorganisms with embedded plasmonic gold nanorods under irradiation by low-intensity NIR laser light was considered. The results of numerical modeling of the optical properties of plasmon nanorods used in the experiments, and the results of multiscale modeling of the parameters of local hyperthermia with various types of distribution of the concentration of plasmon nanoparticles are presented. Found that the process of concentration of nanoparticles, functionalized with human immune globulins IgA and IgG, around the cells of microorganisms with the formation of "clouds" leads to the appearance of a microscale zone of elevated temperature. This ensures a synergistic effect of a multiplicative increase in the volume of the hyperthermia zone. The results of numerical simulation provide a justification for the experimentally observed increase in the bacterium killing ability at laser hyperthermia of the cellular environment doped with functionalized nanoparticles, without a noticeable increment in the recorded average sample temperature when irradiated with a low intensity laser beam of around 100 mW/cm^2.

Keywords: local laser hypertemia, plasmonic gold nanorods, local temperature modeling, Staphylococcus aureus, bacterium killing

1. INTRODUCTION

The methods of local laser hyperthermia of biological tissues and cell suspensions doped with plasmon nanoparticles have received the widest development and distribution in recent decades as an effective tool for the therapeutic treatment of socially significant diseases, including cancer. The localization of thermal effects is ensured by the successful implementation of at least two successive processes. Firstly, the process of delivering plasmonic nanoparticles to the impact zone and ensuring the level of concentration of nanoparticles necessary for a sufficiently intense absorption of laser radiation. Second, by adjusting the resonance of the nanoparticles to a wavelength close to the wavelength of the laser radiation. This allows one to multiple reduce the integral dose of radiation while maintaining the level of hyperthermia of the local area with nanoparticles.

Gold nanoparticles (GNP), due to the high variability of possible forms, modifiable physical properties, including absorption wavelength of plasmon resonance, are of great interest to biomedical science and applications. GNP can act not only as independent active agents, but also as mediators for targeted delivery of drugs and active molecules, but they can also combine these two properties.[1-3] A large number of studies are devoted to the photothermal effects of GNPs in combination with laser radiation on microorganisms, where results were shown to be dependent on the shape and optical properties of the nanoparticles and properties of laser radiation.[3-8]

The use of GNPs as unique units with programmable physicochemical properties as antibacterial agents has several degrees of complication. In the simplest version, GNP are used as carriers of antimicrobial chemicals. For example, Dasari et al. investigated GNPs and gold ion complexes as antibacterial agents for one nonpathogenic strain *E. coli* and three multidrug-resistant strains *E. coli*, *S. typhimurium* and *S. aureus*.[9] It was shown, that Au(I) and Au(III) as chloride are highly toxic to all studied bacterial strains. In work,[7] the effect of environmental diversity in evaluating nanotoxicity to bacteria was established. Authors assessed the toxicity of 4 nm polyallylamine hydrochloride-wrapped gold

[1] anyakunin@mail.ru; phone 7 845 222-2376; fax 7 845 222-2340

Saratov Fall Meeting 2018: Optical and Nano-Technologies for Biology and Medicine, edited by Elina A. Genina, Valery V. Tuchin, Proc. of SPIE Vol. 11065, 1106516 · © 2019 SPIE
CCC code: 0277-786X/19/$18 · doi: 10.1117/12.2531440

nanoparticles to a panel of bacteria from diverse environmental niches. Results demonstrate that simple interactions between nanoparticles and the bacterial cell wall cannot fully account for observed trends in toxicity.

Penders et al. synthesized GNPs of various shapes (spheres, stars and flowers) with similar dimensions, and evaluated for their antibacterial effects toward *S. aureus*.[8] Analysis of the growth curves obtained for 24 h via optical density measurements showed a strong increase in lag time and a decrease in the exponential growth rate upon the addition of 250–500 μg/mL of gold nanostars and gold nanoflowers. Mahmoud et al. have shown the antibacterial activity of gold nanorods suspensions of different surface functionalities against standard strains of *S. aureus* and *P. acnes*.[10] The results demonstrated that cationic polyallylamine hydrochloride nanorods were severely aggregated when exposed to bacterial growth media compared to other GNP suspensions. However, the antibacterial activity of GNR themselves could not be excluded.

The combination of two antibacterial components - antimicrobial substances and photothermal suppression leads to the synergetic effect and increase the destructive efficiency. Mohamed et al. evaluate the efficiency of GNPs and laser combined therapy as antibacterial approaches against *C. pseudotuberculosis* bacteria *in vitro*.[11] Laser light enhanced the antimicrobial activity of gold nanoparticles by at least one fold due to its photothermal combined effect. Review by Mocan et al. summarizes the latest advancements in the field of nanotargeted laser hyperthermia of multidrug resistance bacteria mediated by GNPs.[12] Another review by Amendola et al., focuses on the phenomenon of plasmon resonance, as a basic and most promising phenomenon that occurs during exposure GNPs to laser radiation.[13] The control of the properties of GNPs is achieved by allowing them to conjugate with other substances. GNPs combined with magnetic nanoparticles,[14] polyethylene glycol or polystyrene,[15] graphene oxide[16] or vancomycin[17] have shown more significant antibacterial effect in comparison with pure GNPs.

In order to provide impact only on the targeted microorganisms immunoglobulins are added to GNP carriers.[18-22] The targeting of antibodies in this case will also depend on the architecture and specificity of the labels. In our studies,[23, 24] gold nanorods conjugated with IgA and IgG in combination with NIR (808 nm) laser light were used to damage *S. aureus* microorganisms. The death rate of *S. aureus* after 30 min of laser irradiation reached 97%. The cell suspension maximal temperature was elevated on 26.5°C.

The goal of this paper is to build a theoretical model describing formation of local temperature fields in suspensions of microorganisms with embedded plasmonic gold nanorods under irradiation by low-intensity NIR laser light in order to quantify pathogen killing efficiency and accompanied average heating of bacterial suspensions found in our earlier studies.[23,24]

2. MATERIALS AND METHODS

Two strains of *Staphylococcus aureus* - methicillin-susceptible (MSSA) and methicillin-resistant (MRSA) were chosen as model objects (L.A. Tarasevich GICC, Moscow, Russia).[23, 24] Staphylococci were grown at 37°C on dense nutrient medium (GRM-agar, Obolensk, Russia). The source of infrared radiation was a diode laser (λ = 808 nm), providing power density of 100 mW/cm^2 (LAS, St. Petersburg). All experiments were carried out in CW mode of radiation. To measure the temperature of the solutions a digital multimeter (MY62, Mastech, China) with a measurement error of ± 0.5°C was used.

To study the effectiveness of the photothermal effects of NIR radiation (808 nm), the following colloids of nanorods were added to the suspension of bacterial cells: 1) PEG-coated gold nanorods (Au-PEG); 2) gold nanorods coated with PEG and functionalized by IgA (Au-PEG-IgA); 3) gold nanorods coated with PEG and functionalized by IgG (Au-PEG-IgG) (Fig. 1). The concentration of nanoparticles in the working solutions was 0.4 mM. Nanorods have length of 44 nm and diameter of 10 nm with the absorption maximum in the NIR (800 nm), functionalized with human immune globulins IgA and IgG, were synthesized and used (see left, lower). The killing ability due to hyperthermia (Table 1) up to 97% of microorganism populations by using this nanotechnology was shown (see right, lower).

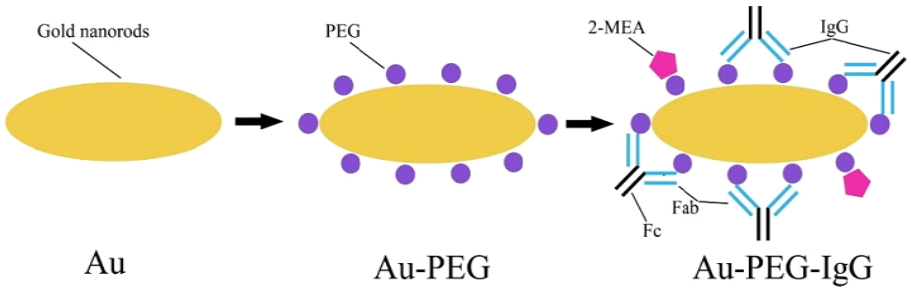

Figure 1. Schematics of fuctionalization of gold nanorods.[23]

The bacterial culture was pre-grown for 24 hours at 37°C on a dense nutrient medium. By the method of serial dilutions, the concentration of microbial cells of 10^4 microbial cells (m.c.) in 1 ml was achieved. 0.1 ml of this suspension was added to 0.9 ml of suspension of nanorods (as well as 0.9 ml of pure saline for control), incubated for 15 min without access of light. Then 0.1 ml of bacterial suspension with concentration 1000 m.c./ml was transferred to cells of polystyrene plate, thus, each compartment contained about 100 bacterial cells.

After pre-incubation, the control solutions with a volume of 0.1 ml were placed in the cells (U-shape, d=6mm) of a sterile polystyrene plate, over which the optical fiber was positioned. Suspension irradiation was performed for 5, 10, 15, and 30 min. At the end of the exposure, the temperature sensor was placed in the cell to measure temperature of the suspension.

To analyze the sensitivity of microbial cells to the overheating of the suspension, a number of control experiments was performed. The 0.5 ml in volume was placed in a polystyrene plate. Incubated without access of light for 30, 60, 90 and 180 min at a temperature of 30, 35, 40, 45 or 50°C. At the end of the measurements, the suspension from the plate and the control samples were transferred to the surface of a dense nutrient medium. Registration of the results was performed by counting the number of colony forming units (CFU) in 24 hours after incubation at 37°C. The control was a suspension of bacteria untreated with nanoparticles and not subjected to irradiation. Each experiment was fulfilled tenfold.

3. EXPERIMENTAL RESULTS AND FORMULATION OF THE PROBLEM

The use of conjugates of nanoparticles with Fc-fragments of immunoglobulins (see Fig.1) led to enhancement of the NIR radiation efficiency for pathogen killing.[23,24] At NIR irradiation of MSSA suspensions with gold nanorods (GNRs) labelled by IgA, the CFU was decreased from 67% for 5 min of laser exposure to 13% for 30 min of laser exposure (Table 1). The mean temperature of the exposed solutions was elevated by 17°C and 22°C in comparison with the temperature of laser-irradiated free of GNRs solutions for 5 min and 30 min exposures, respectively (see Table 2). For MRSA, the CFU was decreased from 74% (5 min) to 6% (30 min) (Table 1), as corresponding GNR suspension overheating was of 16.5°C and 23.5°C for 5 min and 30 min exposures, respectively (see Table 2). For IgG-conjugates, CFU of MSSA decreased to 56% (5 min) and to 5% (30 min) (Table 1). For MRSA strain, a high suppression was found after 15 min-NIR exposure, CFU decreased 4% and to 3% after 30 min (Table 1). The mean temperature of the bacterial suspensions increased up to 24.0–26.5°C for the light exposure of 30 min (see Table 2).

Table 1.The action of NIR (808 nm) light and gold nanorods (GNRs) on MSSA and MRSA colony forming ability (CFU).

Exposure time, min	Laser, 808 nm		Laser, 808 nm + GNRs-PEG		Laser, 808 nm + GNRs-PEG-IgA		Laser, 808 nm + GNRs-PEG-IgG	
	MSSA	MRSA	MSSA	MRSA	MSSA	MRSA	MSSA	MRSA
0	100	100	95	97	92	87	91	86
5	75	81	73	80	67	74	56	73
10	68	75	39	68	33	28	31	26
15	51	70	28	33	21	20	22	4
30	44	56	18	13	13	6	5	3

Table 2. Temporal evolution of the temperature of bacterial suspensions under the action of NIR (808 nm) light

Exposure time, min	T,°C							
	Laser, 808 nm		Laser, 808 nm + GNR-PEG		Laser, 808 nm + GNR-PEG-IgA		Laser, 808 nm + GNR-PEG-IgG	
	MSSA	MRSA	MSSA	MRSA	MSSA	MRSA	MSSA	MRSA
0	20	20	20	20	20	20	20	20
5	20	20	35	34	37	36.5	37	38
10	21	20.5	37	36	38	38.5	41	41.5
15	21.5	21	40	39.5	41	42	43	44
30	23	22.5	42	41	45	46	47	49
Δ	3	2.5	22	21	25	26	27	29
Δ*	-	-	19	18.5	22	23.5	24	26.5

Δ refers to the temperature increase realized from 0 to 30 min;

Δ* refers to the difference in temperature increase between the presence and absence of the nanoparticles

In order to find out whether microorganisms affect the general heating of the medium, experiments on incubation of bacteria in temperature raise conditions without GNPs were carried out. It was found that the viability of microorganisms was not affected by heating of their suspensions up to 50°C during 0.5-3 h. Thus, we may conclude that bacterial cell damage occurs due to photothermal effect mediated by GNPs bound to cell wall via IgA or IgG.

The obtained experimental data on the significant effect of low-intensity laser radiation on the survival rate of cells are only explained by the assumption of the existence of a local temperature difference near plasmonic nanoparticles. The magnitude of this difference must be significant enough so that the Arrhenius damage function during the 1800 s exposure time reaches unity. As follows from the results of the calculation given in Ref.25, this condition (taking into account the monotonous increase in temperature over time) is achieved at a cell temperature of at least 325 K (see Fig. 2).

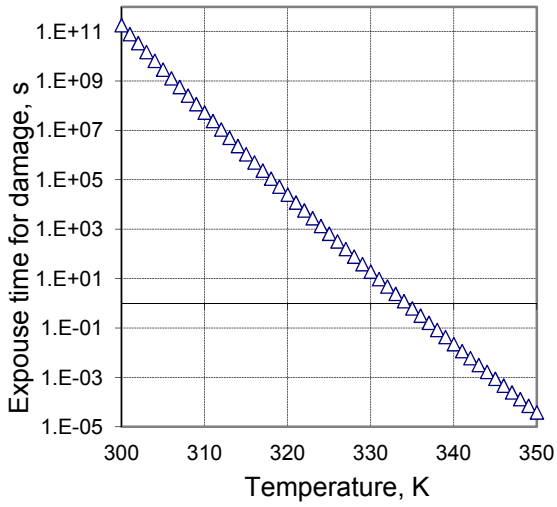

Figure 2. Dependence of the exposure time needed for 100%-damage of a biological material vs. stationary temperature exposure.[25]

On the one hand, the maximal temperature recorded with a thermal imager in experimental studies was 314-322 K, which seemed to indicate the existence of a certain temperature deficit to ensure 100% cell damage. But, on the other hand, the observed cell death indicates the presence of local areas with elevated temperature, apparently associated with the presence of plasmonic nanoparticles or their clusters. Moreover, the spatial scale of these localization zones is so small that they could not be recorded (visualized) in studies conducted with the use of a thermal imager. In recent years,

methods for using the temperature dependence of the spectral characteristics of the upconversion luminescence nanoparticles have been developed to measure the temperature of nanoscale structures.[26-28]

To test the proposed hypothesis in the following sections, we estimate the optical parameters of plasmonic nanorods, determine the level of absorbed power by them, and calculate additional temperature differences due to absorption of laser radiation with an intensity of 100 mW/cm^2.

4. THEORETICAL MODELLING

4.1. Optical parameters of nanorods under 808 nm laser irradiation

Assuming a uniform distribution of nanorods in the sample and, knowing their concentration, we consider a cubic cell with an edge size of 1000 nm as the computational domain. On the boundary surfaces we set the symmetry conditions. When a nanowire is irradiated with a plane wave, the distribution of the optical field in the computational domain and the degree of absorption of the laser beam power will significantly depend on the orientation of the nanorod relative to the direction of the electric field vector of the incident wave. To carry out estimates, we choose the orientation of the nanorod when the absorption is maximal (the semi-major axis coincides with the electric field vector of the wave). The distribution of the magnitude of the electric field vector E_{norm} is shown in Fig. 3

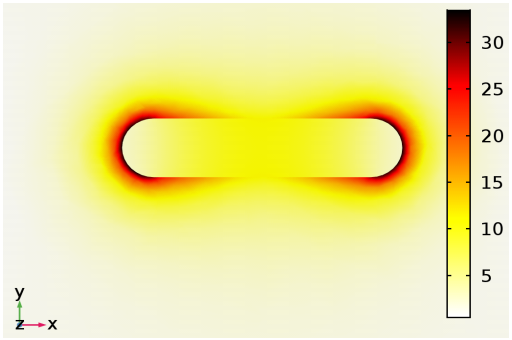

Figure 3. E_{norm} distribution in the nanorod and in the surrounding area (V/m).

Note that in Fig. 3, the maximum of the modulus of the electric field is observed outside the nanorod, in the vicinity of its ends. At the same time, the E_{norm} minimum is localized in the same neighborhood, but inside the nanorod. In the central part of the nanorod, there is a gradual E_{norm} increase zone (distributed maximum) with a level equal to approximately one third of the global maximum. The noted features of the distribution of the field E_{norm} determine the non-uniformity of the specific power absorption, as shown in Fig. 4.

Despite the given levels of specific volumetric absorption power, reaching values of $1.46 \cdot 10^6$ W/cm^3, one should not expect significant temperature differences in the vicinity of the nanorod. Comparison with the results of temperature calculations for the nanospheres given in the Ref. 25 shows the need to increase the intensity of laser radiation by at least 5 orders of magnitude in order to achieve additional heating of 1 K nanosphere with a diameter of 20 nm.

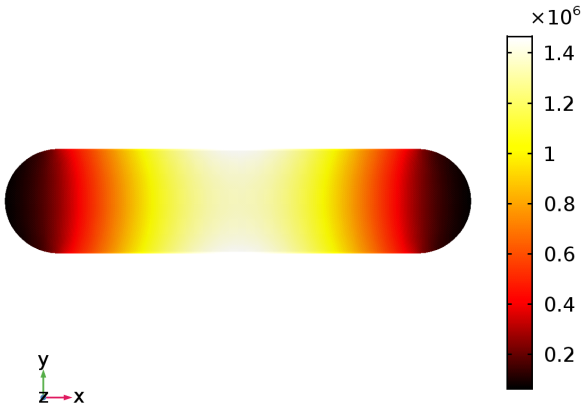

Figure 4. Distribution of specific absorption power (W/cm^3) in the nanorods.

4.2. Local hyperthermia by a single nanorod

The low intensity of laser radiation facilitates the use of a multiscale simulation method,[29] since due to the small temperature difference in the macroscale region (the temperature is recorded experimentally), we can limit ourselves to considering the temperature field in the nanoscale of the nanorod.[30]

To estimate the additional local heating due to the heat transfer to the biological environment of the absorbed laser power in the nanorod, the stationary heat conduction problem was solved in the same size region as was used in the previous section to solve the electrodynamic problem of the optical field distribution. A specific feature of the temperature differential field obtained was the angular anisotropy of its change in the direction normal to the surface of the nanorod. As can be seen from the data in Fig. 5, the temperature drop curve in the vicinity of the end of the nanorod (along the long axis) has a sharper drop than in the vicinity of the middle part of the nanorod (along the short axis). Thus, the temperature difference at the same distance of 10 nm from the surface of the nanorod in the first case is 1.25 times higher than in the second. As the nanorod moves away from the surface, the temperature field becomes close to symmetrical, and at a distance of 150 nm their difference in temperature becomes negligible.

Due to the high thermal conductivity of gold compared to the thermal conductivity of the biological environment, the actual nanorod is an isothermal volume. The maximum temperature gradient of a nanorod-biological medium is no more than $2.4 \cdot 10^{-5}$ K, which, of course, cannot cause a noticeable increment in the Arrhenius function of damage and affect cell survival. The result obtained corresponds to the concentration of nanorods $1 \cdot 10^{12}$ cm^{-3}. It can be shown that increasing the concentration of nanorods evenly throughout the volume will not lead to a qualitative change in the situation with local temperature differences while maintaining the same level of intensity of laser radiation. Thus, an increase in concentration by two orders of magnitude (the average distance between nanoparticles decreases from 1000 to 220 nm) leads only to a 10% decrease in local temperature differences in the vicinity of nanoparticles. However, an increase in the concentration of nanoparticles is accompanied by a proportional increase in the rate of increase in the average temperature of the biological environment, since it is determined by the level of integrated absorbed power.

Thus, the assumption of the existence of a significant temperature difference in a nanoscale neighborhood of solitary nanorods is not confirmed, and the experimentally observed effect of increasing the killing ability of cells during laser low-intensity irradiation of the studied biological medium with functionalized nanoparticles requires a different explanation.

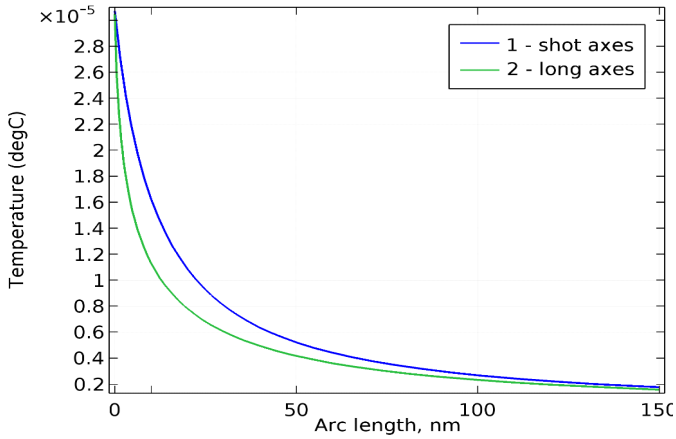

Figure 5. Dependences of temperature increments along the short and long axes of the nanorod: the zero of the Arc length of the nanorod corresponds to a point on the surface of the nanorod; the power absorbed by the nanorod corresponds to a 808 nm-laser beam irradiation with an intensity of 0.1 W/cm^2.

4.3. Local hyperthermia induced by a cloud of nanorods

As a possible reason for the local temperature increase, the hypothesis of concentrating of nanorods, functionalized with human immune globulins IgA and IgG, around the microorganism cell with the formation of a kind of "cloud" in its vicinity is considered. The size of such a cloud and the concentration of nanoparticles in it are the two parameters that determine the cell temperature inside the cloud. Actually, an increase in the overall concentration of nanoparticles, as was shown in the previous section, does not lead to any noticeable additional temperature difference. With a decrease in the distance between adjacent nanorods, the local temperature field becomes homogeneous. This follows from the analysis of the results in Fig. 5. However, an ensemble of nanoparticles with a higher concentration may result in the occurrence of heat flux and, accordingly, the appearance of temperature heterogeneity if this ensemble occupies an area of higher dimensionality compared to the size of nanoparticles. In particular, this effect was investigated numerically in Ref. 29 and the analytical solution for the particular case is given in Ref.31

The possibility of nanoparticles for clusterization around bacteria is well demonstrated.[32,33] In Fig. 6a, TEM images of an *E. coli* fragment after incubation with carbon nanotubes (CNTs) is shown,[32] arrows indicate CNT clusters at the bacteria wall in the form of multilayer cloud of nanoparticles. Optical transmission (Fig. 6b) and fluorescence (Fig. 6c) microscopic images of Staphylococcus aureus bacteria after incubation with GNR/hematoporphyrin (HP) composites also well demonstrate that fluorescent nanoparticles are concentrated around bacteria showing a very bright fluorescence.[33] In contrast, fluorescence microscopic image of HP solution of the similar concentration as was used to label GNR/HP composites (Fig. 6d) has a very low intensity of fluorescence because of its uniform distribution in space.[33]

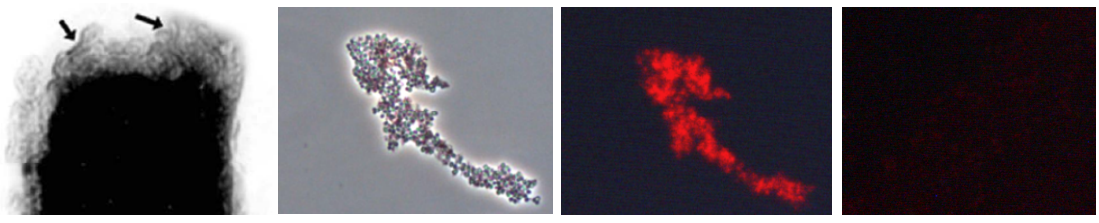

a b c d

Figure 6. Clusterization of nanoparticles around bacteria: TEM images of an *E. coli* fragment after incubation with carbon nanotubes (CNTs),[32] arrows indicate CNT clusters at the bacteria wall; transmission (b) and fluorescence (c) microscopic images of *Staphylococcus aureus* bacteria after incubation with GNR/hematoporphyrin (HP) composites;[33] fluorescence microscopic image of HP solution of the similar concentration as for case (c) (d).

As a model example, we consider the solution of the problem of the stationary temperature field of the system "cell-cloud of nanorods-biological environment". We represent the cell as an object in the form of a spheroid with semiaxes of 750 and 500 nm. Having determined the absorption cross section of a nanorod when irradiated with a laser with a wavelength of 808 nm, we vary the size of the cloud of nanoparticles around the cell and their number in the cloud so as to provide the calculated cell temperature increment at the level of 3-9°C. We assume that the intensity of the incident laser beam remains unchanged and corresponds to the experimental level of 0.1 W/cm^2. In accordance with the multiscale simulation method,[29,30] the intensity of heat sources in the cloud volume was assumed to be equal to the average integral value, equal to the ratio of the integrated absorbed laser radiation power to the cloud nanoparticles.

The results of the numerical experiment showed that the cloud thickness of the nanoparticles should be large enough so that the volume concentration of the nanoparticles does not exceed 15%. Otherwise, it is necessary to consider a large cluster with the participation of a large number of nanoparticles and it is necessary to take into account multiple scattering. This greatly complicates the computational model, without guaranteeing an adequate solution.

Within the framework of the above approach, it was obtained that a cloud with a diameter of 5 μm, surrounding the cell and containing $3.8 \cdot 10^8$ nanorods, satisfies the formulated requirements and provides an additional increase in the cell temperature by 3°C (taking into account the Gaussian intensity distribution in the laser beam, it can increase by 2-3 times). The distribution of temperature difference is presented in Fig. 7. Bold black curves denote cell boundaries and clouds of nanoparticles around it. Equipotential temperature difference is indicated by colored isolines indicating the level of temperature difference. It is seen that the cell and a significant part of the cloud are almost isothermal. At the maximum temperature increment level of 3°C, the temperature change inside the region with a diameter of 3.4 μm (cell + part of the cloud) does not exceed 0.1° C. It should be noted that the structure described has a different spatial scale of temperature inhomogeneity – at the level of several micrometers.

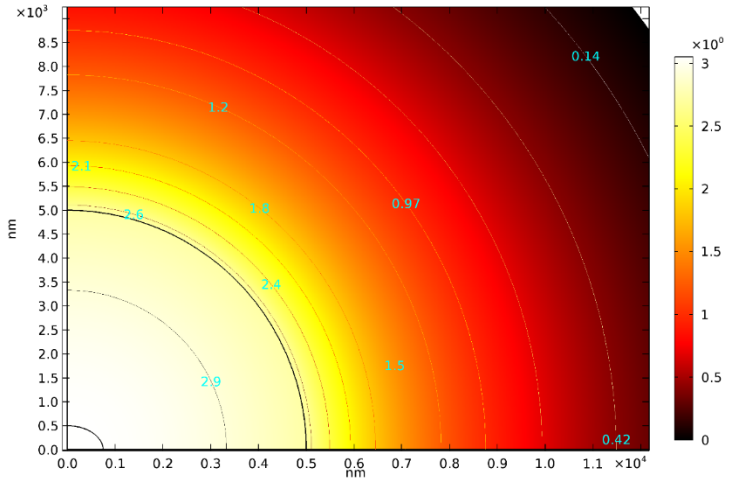

Figure 7. Temperature increment distribution in a cell surrounded by a cloud with a diameter of 5 μm and containing $3.8 \cdot 10^8$ nanorods; the magnitude of the power absorbed by the cloud corresponds to a 808 nm-laser beam irradiation with an intensity of 0.1 W/cm^2.

An analysis of the results of modeling the temperature field allows us to state that the described mechanism for the occurrence of local temperature inhomogeneities of a significant level, the spatial dimension of which is small and cannot be detected by standard temperature sensors, provides a qualitative justification for the experimentally observed efficiency of using low-intensity laser hyperthermia using functionalized gold plasmon resonance nanorods.

5. CONCLUSION

Under conditions of low-intensity laser irradiation (at a level of 0.1 W/cm^2), single nanorods are not able to provide appreciable local hyperthermia.

However, the cloud of nanorods not only increases the additional heating to a significant level (3°C), but also increases the scale of localization of temperature field to a micrometer scale.

ACKNOWLEDGEMENTS

This study was supported by the Research Program of Institute of Precision Mechanics and Control of the RAS and the Program of Basic Research of the Presidium of the RAS No. 32 "Nanostructures: Physics, Chemistry, Biology, Technology Basics". Authors are thankful to Fulvio Ratto for fruitful discussions.

REFERENCES

[1] Hamblin, M.R. "Antimicrobial photodynamic inactivation: a bright new technique to kill resistant microbes", Current Opinion in Microbiology 33, 67-73 (2016).
[2] Wainwright, M., Maish,T., Nonell, S., Plaetzer, K., Almeida, A., Tegos, G., Hamblin, M. R. "Photoantimicrobials-are we afraid of the light?", The Lancet Infectious Disease 17(2), 49-55 (2017).
[3] Moon, K.-S., Park, Y.-B., Ji-Myung, Bae, J.-M., Oh, S. "Near-infrared laser-mediated drug release and antibacterial activity of gold nanorod–sputtered titania nanotubes", J. of Tissue Engineering 9, 1-9 (2018).
[4] Karimi, M., Zangabad, P. S., Ghasemi, A., Amiri, M., Bahrami, M., Malekzad, H., Asl, H.G., Mahdieh, Z., Bozorgomid, M., Ghasemi, A., Reza, M., Boyuk, R.T., Hamblin, M.R. "Temperature-Responsive Smart Nanocarriers for Delivery Of Therapeutic Agents: Applications and Recent Advances", ACS Appl. Mater. Interfaces 8, 21107-21133 (2016).
[5] Hamblin, M.R. "Mechanisms and applications of the anti-inflammatory effects of photobiomodulation", AIMS Biophys. 4, 337-361 (2017).
[6] Yin, R., Agrawa, T., Khan, U., Gupta, G.K., Rai, V., Huang, Y.-Y., Hamblin, M.R. "Antimicrobial photodynamic inactivation in nanomedicine: small light strides against bad bugs", Nanomedicine (Lond). 10(15), 2379-2404 (2015).
[7] Buchman, J.T., Rahnamoun, A., Landy, K.M., Zhang, X., Vartanian, A. M., Jacob, L.M., Murphy, C.J., Hernandez, R., Haynes, C." Using an environmentally-relevant panel of Gram-negative bacteria to assess the toxicity of polyallylamine hydrochloride-wrapped gold nanoparticles", Environ. Sci.: Nano 5, 279-288, (2018).
[8] Penders, J., Stolzoff, M., Hickey, D.J., Andersson, M., Webster, T.J. "Shape-dependent antibacterial effects of non-cytotoxic gold nanoparticles", Int. J. of Nanomedicine 12, 2457-2468 (2017).
[9] Dasari, S., Zhang, Y., Yu, H. "Antibacterial Activity and Cytotoxicity of Gold (I) and (III) Ions and Gold Nanoparticles", Biochem. Pharmacol. 4(6), 199-206 (2015).
[10] Mahmoud, N. N., Alkilany, A.M., Khalil, E.A., Al-Bakri, A. G. "Antibacterial activity of gold nanorods against Staphylococcus aureus and Propionibacterium acnes: misinterpretations and artifacts", Int. J. of Nanomedicine 12, 7311-7322 (2017).
[11] Mohamed, M.M., Fouad, S.A., Elshoky, H.A., Mohammed, G.M, Salaheldin, T.A. "Antibacterial effect of gold nanoparticles against Corynebacterium pseudotuberculosis" Int. J. of Veterinary Science and Medicine 5(1), 23-29 (2017).
[12] Mocan, L., Tabaran, F.A., Mocan, T., Pop, T., Mosteanu, O., Agoston-Coldea, L., Matea, C.T., Gonciar, D., Zdrehus, C., Iancu, C. "Laser thermal ablation of multidrug-resistant bacteria using functionalized gold nanoparticles", Int. J Nanomedicine 12, 2255-2263 (2017).
[13] Amendola, V., Pilot, R., Frasconi, M., Maragò, O.M., Iatì, M.A. "Surface plasmon resonance in gold nanoparticles: a review", J. of Physics: Condenser Matter 29(20), 203002 (2017).
[14] Mohankandhasamy R., Su S.L, Dong K.Y., Kwangmeyung K. "Magnetic, optical gold nanorods for recyclable photothermal ablation of bacteria", J. Mater. Chem. B 2, 981-989 (2014).
[15] Mahmoud, N.N, Alkilany, A.M, Khalil, E.A., Al-Bakri, A.G. "Nano-Photothermal ablation effect of Hydrophilic and Hydrophobic Functionalized Gold Nanorods on Staphylococcus aureus and Propionibacterium acnes", Scientific Reports 8, 6881-1-10 (2018).
[16] Luo, J., Deng, W., Yang, F., Wu, Z., Huang, M., Gu, M. "Gold nanoparticles decorated graphene oxide/nanocellulose paper for NIR laser-induced photothermal ablation of pathogenic bacteria", Carbohydrate Polymers 198, 206-214 (2018).
[17] Wang, S.-G., Chen, Y.-C., Chen, Y.-C. "Antibacterial gold nanoparticle-based photothermal killing of vancomycin-resistant bacteria", Nanomedicine 13, 1405-1416 (2018).
[18] Millenbaugh, N.J, Baskin, J.B., De Silva, M.N., Elliott, W.R., Glickman, R.D. "Photothermal killing of Staphylococcus aureus using antibody-targeted gold nanoparticles", Int. J Nanomedicine 10, 1953-1960 (2015).

[19] Mocan, L., Matea, C., Tabaran, F.A., Mosteanu, O., Pop, T., Puia, C., Agoston-Coldea, L., Gonciar, D., Kalman, E., Zaharie, G., Iancu, C., Mocan, T. "Selective in vitro photothermal nano-therapy of MRSA infections mediated by IgG conjugated gold nanoparticles", Scientific Reports 6, 39466 (2016).
[20] Meeker, D.G, Jenkins, S.V., Miller, E.K, Beenken, K.E., Loughran, A.J., Powless, A., Muldoon, T.J., Galanzha, E.I., Zharov, V.P, Smeltzer, M.S, Chen, J. "Synergistic Photothermal and Antibiotic Killing of Biofilm-Associated Staphylococcus aureus Using Targeted Antibiotic-Loaded Gold Nanoconstructs", ACS Infect. Dis. 2(4), 241-250 (2016).
[21] Hu, D., Li, H., Wang, B., Ye, Z., Lei, W., Jia, F., Jin, O., Ren, K-F., Ji, J. "Surface-adaptive gold nanoparticles with effective adherence and enhanced photothermal ablation of methicillin-resistant *Staphylococcus aureus* biofilm", ACS Nano 11, 9330-9339 (2017).
[22] Centi, S., Ratto, F., Tatini, F., Lai, S., Pini, R. "Polylysine as a functional biopolymer to couple gold nanorods to tumor-tropic cells", J. Nanobiotechnology, 16(50), 1-10 (2018).
[23] Tuchina, E.S., Petrov, P.O., Kozina, K.V., Ratto, F., Centi, S., Pini, R., Tuchin, V.V. "Using gold nanorods labelled with antibodies under the photothermal action of NIR laser radiation on Staphylococcus aureus," Quantum Electronics 44 (7), 683-688 (2014).
[24] Tuchina, E.S., Petrov, P.O., Ratto, F., Centi, S., Pini, R., Tuchin, V.V. "The action of NIR (808nm) laser radiation and gold nanorods labeled with IgA and IgG human antibodies on methicillin-resistant and methicillin sensitive strains of Staphylococcus aureus," Proc. SPIE 9324: Biophotonics and Immune Responses X 93240X, 1-10 (2015).
[25] Yakunin, A. N., Avetisyan, Yu. A., Tuchin, V. V., "Quantification of laser local hyperthermia induced by gold plasmonic nanoparticles," Journal of Biomedical Optics 20(5), 051030(1-9) (2015) https://doi.org/10.1117/1.JBO.20.5.051030
[26] Savchuk, Ol. A., Haro-González, P., Carvajal, J. J., Jaque, D., Massons, J., Aguiló, M., Díaz, F., "Er:Yb:NaY2F5O up-converting nanoparticles for sub-tissue fluorescence lifetime thermal sensing," Nanoscale 6(16), 2040-3364 (2014). DOI: 10.1039/C4NR02305F
[27] Rafiei Miandashti, A., Khosravi Khorashad, L., Govorov, A. O., Kordesch, M. E., Richardson, H. H., "Time-Resolved Temperature-Jump Measurements and Theoretical Simulations of Nanoscale Heat Transfer Using NaYF4:Yb3+:Er3+ Upconverting Nanoparticles," J. Phys. Chem. C (2019). DOI: 10.1021/acs.jpcc.8b11215
[28] Balabhadra, S., Debasu, M. L., Brites, C. D. S., Ferreira, R. A. S., Carlos, L. D., "Upconverting Nanoparticles Working As Primary Thermometers In Different Media," J. Phys. Chem. C 121 (25), 13962-13968 (2017). DOI: 10.1021/acs.jpcc.7b04827
[29] Avetisyan, A. Yu., Yakunin, A. N., Tuchin, V. V., "On the problem of local tissue hyperthermia control: multiscale modelling of pulsed laser radiation action on a medium with embedded nanoparticles," Quantum Electronics 40(12), 1081–1088 (2010). http://dx.doi.org/10.1070/QE2010v040n12ABEH014502
[30] Avetisyan, Yu. A., Yakunin, A. N., Tuchin, V. V., "Thermal energy transfer by plasmon-resonant composite nanoparticles at pulse laser irradiation," Appl. Opt. 51(10), C88-C94 (2012). DOI: 10.1364/AO.51.000C88
[31] Avetisyan, Yu. A., Yakunin, A. N., Bykov, A. A., Tuchin, V. V., "The modeling of local distribution of the temperature photo-induced by ensemble of nanoparticles," Proc. of 2016 Int. Conf. Laser Optics (LO) S2-48-S2-48 (2016). DOI: 10.1109/LO.2016.7550015
[32] Zharov, V.P., Galanzha, E.I., Shashkov, E.V., Kim, J.-W., Khlebtsov, N.G., and Tuchin, V.V. "Photoacoustic flow cytometry: principle and application for real-time detection of circulating single nanoparticles, pathogens, and contrast dyes *in vivo*," J. Biomed. Opt. 12 (5), 051503 (2007).
[33] Khlebtsov, B. N., Tuchina, E. S., Khanadeev, V. A., Panfilova, E. V., Petrov, P. O., Tuchin, V. V., and Khlebtsov, N. G. "Enhanced photoinactivation of Staphylococcus aureus with nanocomposites containing plasmonic particles and hematoporphyrin," J. Biophotonics 6 (4), 338–351 (2013). DOI 10.1002/jbio.201200079.